Journal of Alloys and Compounds 514 (2012) 40–44

Contents lists available at SciVerse ScienceDirect

Journal of Alloys and Compounds

journal homepage: www.elsevier.com/locate/jallcom

Electrical and thermal transport properties of Pb-based chalcogenides: PbTe, PbSe, and PbS

Yan-Ling Pei [a,b,*], Yong Liu [c]

[a] School of Materials Science and Engineering, Beihang University, Beijing 100191, China
[b] Beijing Key Laboratory for Advanced Functional Materials and Thin Film Technology, Beihang University, Beijing 100191, China
[c] School of Metallurgical and Ecological Engineering, University of Science and Technology Beijing, Beijing 100083, China

ARTICLE INFO

Article history:
Received 25 September 2011
Received in revised form 8 October 2011
Accepted 13 October 2011
Available online 3 November 2011

Keywords:
Lead chalcogenide
Electrical resistivity
Seebeck coefficient
Thermal conductivity

ABSTRACT

Electrical and thermal transport properties of lead-based chalcogenides (PbTe, PbSe, and PbS) were studied with special emphasis on the lattice and the bipolar thermal conductivity. Both electrical resistivity and Seebeck coefficient show the transport behaviors related to the intrinsic excitation that determined by the band gap, power factors at room temperature reach 12 μW cm^{-1} K^{-2}, 14 μW cm^{-1} K^{-2}, and 16 μW cm^{-1} K^{-2} for PbS, PbSe and PbTe, respectively. PbTe shows the lowest total thermal conductivity, and PbS shows the highest total thermal conductivity, in which the bipolar thermal conductivity is proportional to the width of band gap, these contributions at 723 K were estimated to be 2.2%, 3.1%, and 1.1% for the PbTe, PbSe and PbS, respectively. This study demonstrates the possibility to enhance *ZT* value by the suppression of bipolar thermal conductivity by tuning the width of band gap, also indicates that inexpensive and earth-abundant PbSe and PbS would be promising alternative for PbTe in the thermoelectric applications.

1. Introduction

Thermoelectric (TE) technology is a kind of energy conversion technology between heat and electricity, which includes power generation and electronic refrigeration. The efficiency of TE devices is strongly associated with the dimensionless figure of merit (*ZT*) of a given TE material, defined as $ZT = (\alpha^2/\rho\kappa)T$, where α, ρ, κ, and T are the Seebeck coefficient, the electrical resistivity, the thermal conductivity, and the absolute temperature, respectively. Therefore, low electrical resistivity ρ (corresponding to low Joule heating), large Seebeck coefficient α (corresponding to large potential difference), and low thermal conductivity κ (corresponding to large temperature difference) are necessary for high-performance TE materials [1,2].

Lead-based chalcogenides, PbTe, PbSe, and PbS, have been extensively studied by experiments over the past several decades due to their potential applications as thermoelectric energy converters and electronic devices. As narrow-gap semiconducting IV–VI compounds, lead chalcogenides exhibit outstanding electrical transport properties, meanwhile, they exhibit low thermal conductivities at high temperature, which is unusual for simple structured materials (NaCl structure). These unique features in electron and heat transport have made them practical TE materials for a long time. To date, several classes of bulk materials with high *ZT* values have been discovered, including nanostructured BiSbTe alloys [3], $AgPb_mSbTe_{m+2}$ [4], Tl doped PbTe [5], $(AgSbTe_2)_{1-x}(GeTe)_x$ [6], Na doped $PbTe_{1-x}Se_x$ [7], PbTe–SrTe [8]. These materials show high performance at room and middle temperature range, however, the common feature of these materials is that they contain significant amount of Te, which is a scarce element in the crust of the earth. Hence the Te price is likely to rise sharply if Te-based TE materials reach mass markets. A broad search for more inexpensive alternatives is therefore required and the examples are the exploratory of PbSe and PbS [9–12].

In this paper, electrical and thermal transport properties of lead chalcogenides PbTe, PbSe, and PbS have been focused with an emphasis on the lattice thermal conductivity and the bipolar thermal conductivity. These studies will give broad researching information to explore inexpensive lead-based chalcogenide materials, and suggest that PbSe and PbS would be very promising candidates for the thermoelectric power generation applications.

2. Experimental

PbTe (PbSe and PbS) were prepared by using mixing elemental Pb and Te (Se and S) inside carbon-coated silica tubes, the tubes were then evacuated to a base pressure of ~10^{-4} torr, fused, slowly heated to 723 K in 12 h, and then heated to 1323 K (1373 K and 1423 K) in 7 h, soaked at this temperature for 6 h and subsequently air quenching to room temperature. Phase identification and grain orientation of the samples were analyzed by X-ray diffraction (XRD, CuKα,

* Corresponding author at: School of Materials Science and Engineering, Beihang University, Beijing 100191, China. Tel.: +86 10 82338173.
E-mail address: peiyanling@mse.buaa.edu.cn (Y.-L. Pei).

0925-8388/$ – see front matter © 2011 Elsevier B.V. All rights reserved.
doi:10.1016/j.jallcom.2011.10.036

Bruker D8, Germany). Room temperature optical diffuse reflectance measurements were performed at room temperature using a Shimadzu UV-3101 PC double-beam, double-monochromator spectrophotometer operating in the 200–2500 nm region. The reflectance versus wavelength data generated, were used to estimate the band gap by converting reflectance to absorption data according to Kubelka–Munk equations: $\alpha/S = (1-R)^2/2R$, where R is the reflectance and α and S are the absorption and scattering coefficients, respectively. The Hall coefficients, R_H, of the samples were measured at 323 K using a physical property measurement system (PPMS-9T, Quantum Design Inc., USA), and a magnetic field of 2T and electrical current of 30 mA were applied. The longitudinal and transverse acoustic velocities were measured by an ultrasonic instrument (Ultrasonic Pulser/Recever Model 5900 PR, Panametrics, USA) and the elastic constants were then calculated from the measured velocities [13]. The Seebeck coefficient and electrical resistivity were measured at 300–723 K in a helium atmosphere using a Seebeck coefficient/electric resistance measuring system (ZEM-2, Ulvac-Riko, Japan). The thermal diffusivity coefficient (D) was measured using the laser flash method (NETZSCH, LFA427, Germany). The specific heat (C_p) was measured using a thermal analyzing apparatus (Dupont 1090B, USA), the C_p results show good agreement with the reported values [14]. The density (d) of the sample was measured by the Archimedes method. The thermal conductivity (K) was calculated from the product of thermal diffusivity, specific heat and density, $K = DC_p d$.

3. Results and discussion

As shown in Fig. 1(a), all the XRD patterns show single phases without any impurity phases, and all the major Bragg peaks can be indexed in the NaCl structure type. It also can be seen that all the Bragg peaks for PbTe, PbSe and PbS shift to high angel direction from Te to S, this is in a good agreement with the decreasing lattice

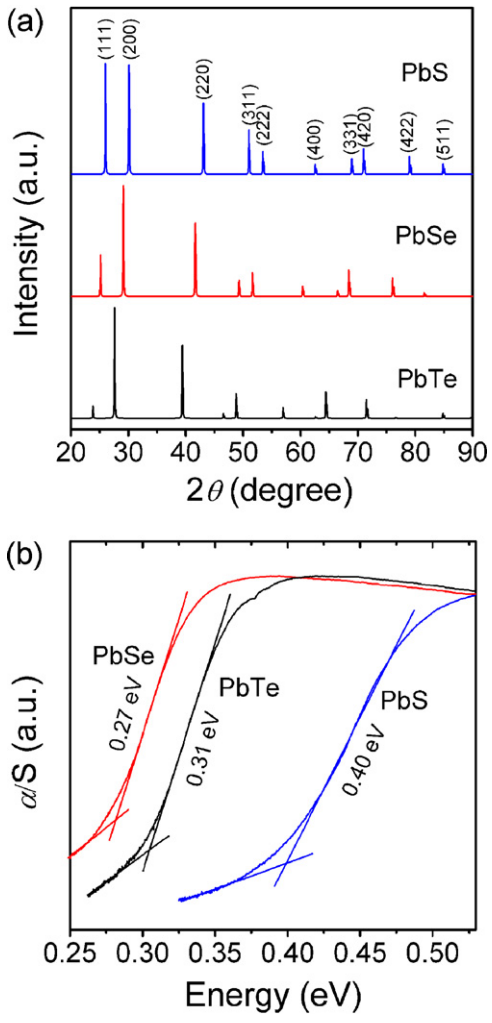

Fig. 1. (a) Powder XRD and (b) electronic absorption spectra obtained from diffuse reflectance infrared spectroscopy measurements of PbTe, PbSe, and PbS.

Table 1
Physical properties parameters at room temperature for PbTe, PbSe, and PbS.

Parameters		PbTe	PbSe	PbS
Lattice constant	a (Å)	6.454	6.121	5.936
Density of mass	ρ (g/cm^3)	8.24	8.27	7.614
Gruneisen parameter	γ	1.96	2.23	2.52
Longitudinal sound velocity	v_l (m/s)	3596	3820	4080
Transverse sound velocity	v_s (m/s)	1610	1720	1840
Average sound velocity	v_a (m/s)	1770	1910	2040
Young's modulus	E (GPa)	27.7	36.9	39.3
Debye temperature	θ_D (K)	136	141	145
Carrier concentration	n (10^{18}/cm^3)	2.6	3.5	1.2
Carrier mobility	μ (cm^2/V s)	383	475	538
K_{lat}/κ_{tot} at RT	%	90.3	91.6	94.8
$\kappa_{lat}/\kappa_{tot}$ at 723 K	%	87.9	90.3	97.8
K_{bi}/κ_{tot} at 723 K	%	2.2	3.1	1.1

parameters for these lead chalcogenides, as listed in Table 1. In Fig. 1(b), the electronic absorption spectra are shown as a function of photon energy for PbTe, PbSe and PbS. Here the band gaps are 0.31 eV, 0.27 eV, and 0.40 eV for PbTe, PbSe and PbS respectively. These are in agreement with the reported values of the optical band gap from spectroscopic absorption measurements [9,12].

Fig. 2 shows the electrical transport properties as a function of temperature for PbTe, PbSe and PbS, including electrical resistivity, Seebeck coefficient, and power factor. Fig. 2(a) shows that all the electrical resistivity shows a metallic transport behavior dependent temperature, which increases with increasing temperature, also indicates that PbSe shows the lowest electrical resistivity values, and PbS shows the highest electrical resistivity values at room temperature among all the lead chalcogenides. In Fig. 2(b) all the negative Seebeck coefficients indicate all samples are n-type, and major carrier is predominated by electrons. The absolute values of the Seebeck coefficients for PbS show an increasing trend with increasing temperature, but the Seebeck coefficients of PbSe and PbS show up-turn curves. It should be noted that the up-turn point of PbSe is about 600 K, which is lower than that (650 K) of PbTe. All the samples are supposed as intrinsic conductors since no carrier variations of by dopants. Therefore, these up-turn behaviors should be related to the intrinsic excitation of a given narrow-band semiconductors. Various behaviors in electrical resistivity and Seebeck coefficient are in good agreement with the carrier concentration and mobility, as summarized in Table 1. Present electrical resistivity and Seebeck coefficient can be explained by the band gap of these lead chalcogenides. The band gap is a major factor determining the electrical resistivity, can reflect the how difficulty for the carrier (electrons or holes) requires a specific minimum amount of energy for the transition. The band gap is equivalent to the energy required to jump to the conduction band by absorbing energy. Meanwhile, for the Seebeck coefficient, the intrinsic excitation temperature will increase with increasing band gap, present examples are PbTe with band gap of 0.32 eV shows the intrinsic excitation temperature of 650 K, PbSe with band gap of 0.27 eV shows the intrinsic excitation temperature of 600 K. All the lead chalcogenides samples peak power factors at room temperature, and show a decrease dependent temperature trend. Namely, power factors at room temperature are 12 μW cm^{-1} K^{-2}, 14 μW cm^{-1} K^{-2}, and 16 μW cm^{-1} K^{-2} for PbS, PbSe and PbTe, respectively, as shown in Fig. 2(c).

Fig. 3 shows the thermal diffusivity, specific heat capacity, and total thermal conductivity as a function of temperature for PbTe, PbSe, and PbS. It can be seen that thermal diffusivities and specific heat capacities in the entire temperature range show inverse dependence on the mass of atom, i.e., PbTe < PbSe < PbS. Fig. 3(a) indicates that the thermal diffusivities of lead chalcogenides evidences inverse temperature dependence in the entire temperature ranges from room temperature to 723 K. As shown in Fig. 3(b), the

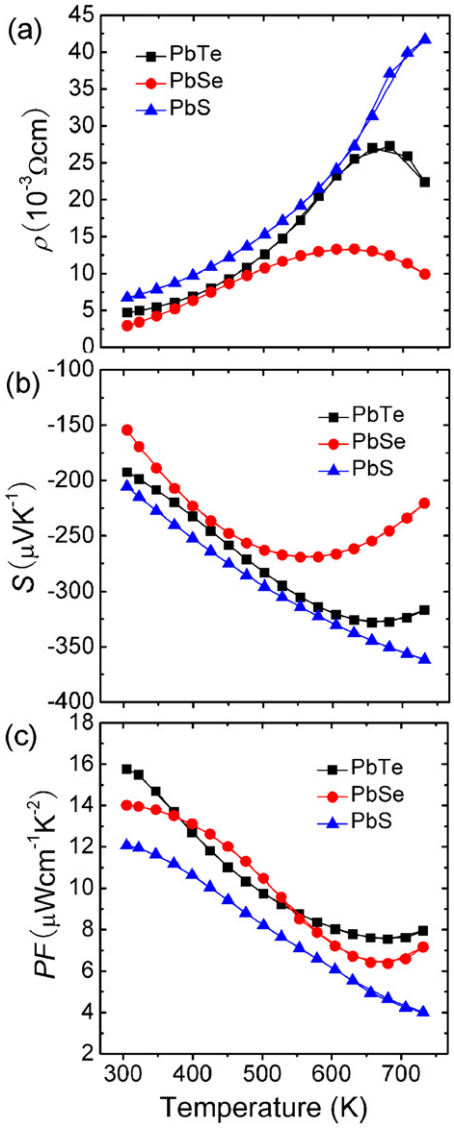

Fig. 2. (a) Electrical resistivity, (b) Seebeck coefficient, and (c) power factor as a function of temperature for PbTe, PbSe, and PbS.

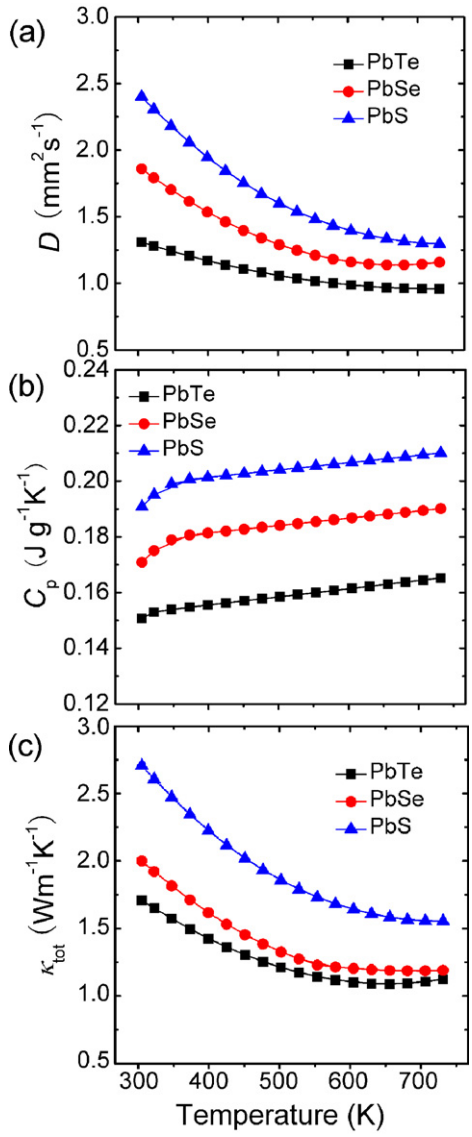

Fig. 3. (a) Thermal diffusivity, (b) specific heat capacity, and (c) total thermal conductivity as a function of temperature for PbTe, PbSe, and PbS.

specific heat capacities of lead chalcogenides have nearly linear temperature dependence, i.e., $C_p \propto T$. The total thermal conductivity of lead chalcogenides shows decreasing temperature dependence, PbTe shows the lowest thermal conductivity, and PbS shows the highest thermal conductivity in the entire temperature, as shown in Fig. 3(c). The thermal conductivity can be determined by the transport behaviors of carriers, especially for phonon, thermal conductivity for different materials has a strong dependence with their sound speeds. Sound speeds are mainly associated with atomic bond strength, which can be scaled by Young's modulus. Phonon will transport slowly inter crystal structure if the bonding strength between atoms is weaker, i.e., Van der Waals bonding strength < ionic bonding strength < covalence bonding strength. The strength of these bonding can be determined by Young's modulus, this means thermal conductivity is proportional to Young's modulus [14–16]. To compare and examine the thermal conductivities of lead chalcogenides, we performed ultrasonic pulse echo measurement. The longitudinal (v_l) and transverse (v_s) sound velocities can be evaluated by the ultrasonic pulse echo measurement.

The average sound velocity (v_a) is given using the following expression [15]:

$$v_a = \left(\frac{1}{3} \left[\frac{1}{v_l^3} + \frac{2}{v_s^3} \right] \right)^{-1/3} \quad (1)$$

Young's modulus (E) and the total thermal conductivity (κ_{tot}) can be calculated from the sound velocity as follows [16]:

$$E = \frac{\rho v_s^2 (3v_l^2 - 4v_s^2)}{(v_l^2 - v_s^2)} \quad (2)$$

$$\kappa_{tot} \propto \frac{\rho^{1/6} E^{1/2}}{(M/m)^{2/3}} \quad (3)$$

where ρ is the sample density, M is the atomic weight of the molecule of the compound, and m is the number of atoms in the molecule. We calculated the material's average sound velocity, Young's modulus, and Debye temperature, respectively, all the data are listed as Table 1. As indicated by Eqs. (2) and (3), the total thermal conductivity of lead chalcogenides increases from Te to S, i.e., PbTe < PbSe < PbS, this can be explained by the increasing Young's

modulus, deceasing atomic weight of the molecule of the compound even though slight decrease in sample density. Here it is worth pointing out that the total thermal conductivity for these pristine lead chalcogenides is predominated by the lattice thermal conductivity. Namely, the ratios of $\kappa_{lat}/\kappa_{tot}$ at temperature are 90.3%, 91.6% and 94.8% for PbTe, PbSe and PbS, respectively, and those at 723 K are 87.9%, 90.3% and 97.8% for PbTe, PbSe and PbS, respectively, as listed in Table 1.

The total thermal conductivity κ_{tot} includes a sum of the electronic κ_{ele} and lattice thermal conductivity κ_{lat}. The electronic part κ_{ele} is inverse proportional to the electrical resistivity ρ through the Wiedemann–Franz relation, $\kappa_{ele} = LT/\rho$, where L is the Lorenz number [17]. Generally, the lattice thermal conductivity κ_{lat} can be estimated by directly subtracting κ_{ele} from κ_{tot} with using:

$$L_0 = \frac{\pi^2}{3}\left(\frac{\kappa_B}{e}\right)^2 = 2.45 \times 10^{-8}\ \mathrm{W\,\Omega\,K^{-2}} \quad (4)$$

Although this may be a good estimation for the lattice thermal conductivity κ_{lat} at room temperature, it does not hold true for metallic materials or for heavily doped semiconductors where a strong change with temperature is observed in the chemical potential [18]. For most thermoelectric materials, the true Lorenz number is in fact lower than L_0 ($2.45 \times 10^{-8}\,\mathrm{W\,\Omega\,K^{-2}}$) especially at high temperature. The Lorenz number depends on the scattering parameter r and will decrease as the reduced Fermi energy η decreases with increasing temperature. The Lorenz number can be given as [19]:

$$L = \left(\frac{\kappa_B}{e}\right)^2 \left(\frac{(r+7/2)F_{r+5/2}(\eta)}{(r+3/2)F_{r+1/2}(\eta)} - \left[\frac{(r+5/2)F_{r+3/2}(\eta)}{(r+3/2)F_{r+1/2}(\eta)}\right]^2 \right) \quad (5)$$

For the Lorenz number calculation, we should get reduced Fermi energy η firstly; the calculation of η can be derived from the measured Seebeck coefficients by using the following relationship:

$$S = \pm\frac{k_B}{e}\left(\frac{(r+5/2)F_{r+3/2}(\eta)}{(r+3/2)F_{r+1/2}(\eta)} - \eta\right) \quad (6)$$

where $F_n(\eta)$ is the nth order Fermi integral,

$$F_n(\eta) = \int_0^\infty \frac{\chi^n}{1+e^{\chi-\eta}}d\chi \quad (7)$$

$$\eta = \frac{E_f}{k_B T} \quad (8)$$

In the above equations, κ_B is the Boltzman constant, e the electron charge, and E_f the Fermi energy. Meanwhile, acoustic phonon scattering ($r = -1/2$) has been assumed as the main carrier scattering mechanism [12,20]. The Lorenz number can be obtained by applying the calculated reduced Fermi energy η and scattering parameter r into Eq. (5). As shown in Fig. 4(a). In addition to the above calculation for Lorenz number, the lattice thermal conductivity κ_{lat} can be estimated by subtracting κ_{ele} from κ_{tot} if no bipolar diffusion exists. If bipolar diffusion takes place the electronic thermal conductivity κ_{ele} will be overestimated when both holes and electrons are present at high temperature, and an extra term (bipolar thermal conductivity, κ_{bi}) then needs to be added to the total thermal conductivity. The minor carriers generated from intrinsic excitation not only decrease the Seebeck coefficient, but also increase thermal conductivity due to the bipolar diffusion in the intrinsic region, especially at high temperatures. Therefore, the total thermal conductivity κ_{tot} is given by:

$$\kappa_{tot} = \kappa_{lat} + \kappa_{ele} + \kappa_{bi} \quad (9)$$

Fig. 4(b) shows the difference of total and electronic thermal conductivity as a function of temperature for PbTe, PbSe, and PbS. The differences of these values are not the truth values of the lattice

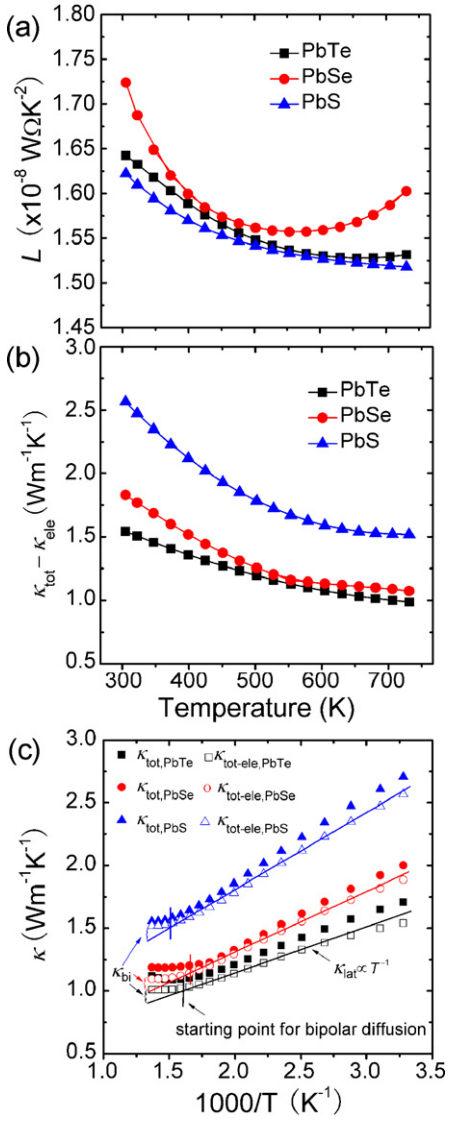

Fig. 4. (a) Lorenz number and (b) difference of total and electronic thermal conductivity as a function of temperature for PbTe, PbSe, and PbS. (c) Component details of thermal conductivity as a function of temperature for PbTe, PbSe, and PbS. The solid line is linearly fitting to the lattice thermal conductivity at temperature ranges from room temperature to 723 K.

thermal conductivity for the PbTe, PbSe and PbS. In order to clarify the contribution of bipolar thermal conductivity κ_{bi} at high temperatures, the κ_{bi} is separated from the κ_{tot} according to the proposed method [21]. The difference, $\kappa_{tot} - \kappa_{ele}$, as a function of T^{-1} for the lead chalcogenides are shown in Fig. 4(c) by the unfilled symbols. Since the acoustic phonon scattering is predominant at low temperatures before starting bipolar diffusion, $\kappa_{tot} - \kappa_{ele}$ equals to κ_{lat}, which is proportional to T^{-1}, the lattice thermal conductivity can be given as follows [22]:

$$\kappa_{lat} = 3.5\left(\frac{k_B}{h}\right)\frac{MV^{1/3}\theta_D^3}{\gamma^2 T} \quad (10)$$

with

$$\theta_D = \frac{h}{k_B}\left[\frac{3N}{4\pi V}\right]^{1/3} v_a \quad (11)$$

where the M is the average mass per atom, V the average atomic volume, θ_D the Debye temperature, and γ the Grüneisen parameter. N is the number of atoms in a unit cell, Slack and Tsoukala

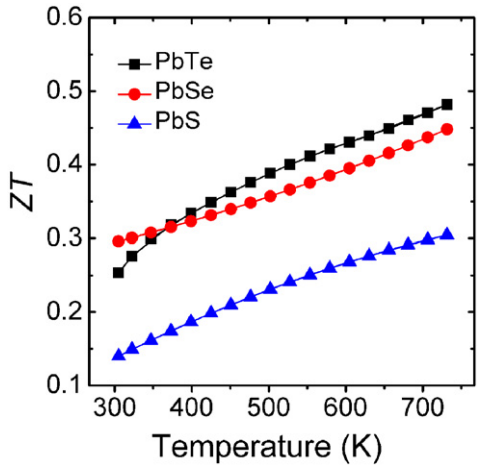

Fig. 5. The dimensionless figure of merit *ZT* as a function of temperature for PbTe, PbSe, and PbS.

used a similar formula to estimate the lattice thermal conductivity of IrSb3 at the Debye temperature [23]. When the measurement temperature was increased to 543 K, the $\kappa_{tot}-\kappa_{ele}$ started to gradually deviate from such a linear relationship between κ_{lat} and T^{-1}. This implies that the bipolar diffusion starts to contribute to the thermal conductivity. The κ_{lat} at high temperatures was estimated by extrapolating the linear relationship between κ_{lat} and T^{-1}, as indicated by the solid line in Fig. 4(c). Hence, κ_{bi} at high temperatures should be equal to $\kappa_{tot}-\kappa_{lat}-\kappa_{ele}$. The contributions of the κ_{bi} to the κ_{tot} at 723 K were estimated to be ~2.2%, ~3.1%, and ~1.1% for the PbTe, PbSe and PbS, respectively. The detailed components of the thermal conductivity for the lead chalcogenides are also summarized in Table 1. It is noted that the contribution of κ_{bi} is proportional to the width of band gap. Here, it may be supposed that the suppression of bipolar thermal conductivity by tailoring the width of band gap (an example is tuning carrier concentration by doping or isoelectrically alloying by narrow band gap materials) will enhance thermoelectric properties.

The dimensionless figure of merit (*ZT*) values for the lead chalcogenides show peaks at 723 K. Namely, *ZT* values are 0.48, 0.45, and 0.3 for the PbTe, PbSe and PbS, respectively, as shown in Fig. 5. These results indicate that PbSe and PbS would be robust alternative for PbTe, and are very promising candidates for the thermoelectric power generation applications.

4. Conclusions

Electrical and thermal transport properties of lead-based chalcogenides (PbTe, PbSe, and PbS) were studied with special emphasis on the lattice and bipolar thermal conductivity, results show that the contribution of bipolar thermal conductivity is proportional to the width of band gap, and occurs with the intrinsic excitation, resulting in an increase in total thermal conductivity at high temperature. It can be assumed that the suppression of bipolar thermal conductivity by tuning the width of band gap would enhance thermoelectric properties. These results also indicate that inexpensive and earth-abundant PbSe and PbS would be robust alternative for PbTe, and are very promising candidates for the thermoelectric power generation applications.

Acknowledgments

This work was financially supported by the Ministry of Sci & Tech of China through a 973-Project, under grant No. 2007CB607505, NSF of China under Grant No. 51025205, and the National High Technology Research and Development Program of China under grant No. 2009AA03Z216.

References

[1] M.G. Kanatzidis, Chem. Mater. 22 (2010) 648.
[2] J.-F. Li, W.-S. Liu, L.-D. Zhao, M. Zhou, NPG Asia Mater. 2 (2010) 152.
[3] B. Poudel, Q. Hao, Y. Ma, Y. Lan, A. Minnich, B. Yu, X. Yan, D. Wang, A. Muto, D. Vashaee, X. Chen, J. Liu, M.S. Dresselhaus, G. Chen, Z.F. Ren, Science 320 (2008) 634.
[4] K.F. Hsu, S. Loo, F. Guo, W. Chen, J.S. Dyck, C. Uher, T. Hogan, E.K. Polychroniadis, M.G. Kanatzidis, Science 303 (2004) 818.
[5] J.P. Heremans, V. Jovovic, E.S. Toberer, A. Saramat, K. Kurosaki, A. Charoenphakdee, S. Yamanaka, G.J. Snyder, Science 321 (2008) 554.
[6] B.A. Cook, M.J. Kramer, X. Wei, J.L. Harringa, E.M. Levin, J. Appl. Phys. 101 (2007) 053715.
[7] Y.Z. Pei, X.Y. Shi, A. LaLonde, H. Wang, L.D. Chen, J.G. Snyder, Nature 473 (2011) 66.
[8] K. Biswas, J.Q. He, Q.C. Zhang, G.Y. Wang, C. Uher, V.P. Dravid, M.G. Kanatzidis, Nat. Chem. 3 (2011) 160.
[9] J. Androulakis, I. Todorov, J.Q. He, D.-Y. Chung, V.P. Dravid, M.G. Kanatzids, J. Am. Chem. Soc. 133 (2011) 10920.
[10] J. Androulakis, L. Yeseul, I. Todorov, D.-Y. Chung, M.G. Kanatzids, Phys. Rev. B 83 (2011) 195209.
[11] H. Wang, Y.Z. Pei, A.D. Lalonde, J.G. Snyder, Adv. Mater. 23 (2011) 1366.
[12] S. Johnsen, J.Q. He, J. Androulakis, V.P. Dravid, I. Todorov, D.-Y. Chung, M.G. Kanatzidis, J. Am. Chem. Soc. 133 (2011) 3460.
[13] M. Asmani, C. Kermel, A. Leriche, M. Ourak, J. Eur. Ceram. Soc. 21 (2011) 1081.
[14] R. Blachnik, R. Igel, Z. Naturforsch. B 29 (1974) 625.
[15] K. Kurosaki, A. Kosuga, H. Muta, M. Uno, S. Yamanaka, Appl. Phys. Lett. 87 (2005) 061919.
[16] K. Kurosaki, H. Uneda, H. Muta, S. Yamanaka, J. Alloys Compd. 376 (2004) 43.
[17] V.I. Fitsul, Heavily Doped Semiconductors, Plenum Press, New York, 1969.
[18] G.S. Kumar, G. Prasad, R.O. Pohl, J. Mater. Sci. 8 (1993) 4261.
[19] W.-S. Liu, Q. Zhang, Y. Lan, S. Chen, X. Yan, Q. Zhang, H. Wang, D. Wang, G. Chen, Z.F. Ren, Adv. Energy Mater. 1 (2011) 577.
[20] L.-D. Zhao, B.P. Zhang, W.-S. Liu, J.-F. Li, J. Appl. Phys. 105 (2009) 023704.
[21] H. Kitagawa, M. Wakatsuki, H. Nagaoka, H. Noguchi, Y. Isoda, K. Hasezaki, Y. Noda, J. Phys. Chem. Solids 66 (2005) 1635.
[22] W.-S. Liu, B.P. Zhang, J.-F. Li, H.L. Zhang, L.-D. Zhao, J. Appl. Phys. 102 (2007) 103717.
[23] G.A. Slack, V.G. Tsoukala, J. Appl. Phys. 76 (1994) 1665.